



Article

Sea Caves and Other Landforms of the Coastal Scenery on Gozo Island (Malta): Inventory and New Data on Their Formation

Stefano Furlani ^{1,*} , Fabrizio Antonioli ², Emanuele Colica ^{3,4} , Sebastiano D'Amico ⁴ , Stefano Devoto ¹ , Pietro Grego ¹ and Timmy Gambin ⁵

¹ Department of Mathematics and Geosciences, University of Trieste, Via Weiss 2, 34127 Trieste, Italy; stefano.devoto@units.it (S.D.); pietro.grego@studenti.units.it (P.G.)

² CNR IGAG, Piazzale Aldo Moro 7, 00185 Rome, Italy; fabrizioantonioli2@gmail.com

³ Research and Planning Unit, Public Works Department, Ministry for Public Works and Planning, Project House, Triq Francesco Buonamici, FRN 1700 Floriana, Malta; emanuele.colica@gov.mt

⁴ Department of Geosciences, University of Malta, MSD 2080 Msida, Malta; sebastiano.damico@um.edu.mt

⁵ Department of Classics and Archeology, Faculty of Arts, University of Malta, MSD 2080 Msida, Malta; timmy.gambin@um.edu.mt

* Correspondence: sfurlani@units.it; Tel.: +39-04-0558-2020

Abstract: Sea caves are a type of cave formed primarily by the wave action of the sea. The coastal scenery of the Gozitan coast is very interesting in that sea caves and other coastal landforms, such as sea arches, develop at the sea level. We mapped seventy-nine semi-submerged sea caves opening at the sea level, five completely submerged sea caves, seven sea arches, one sea stack, and one shelter around the coast of Gozo, mainly in the Western and Eastern parts of the island, due to favorable lithological and topographical conditions. Additionally, we surveyed the topography of the emerged part of nine sea caves using the iPhone build-in LiDAR sensor, and eight sea caves in the submerged part using SCUBA equipment. This inventory represents the most detailed example of a database of coastal caves and related forms in the Mediterranean, mainly sourced from a swimming survey along the entire island. Thanks to the combination of outputs of the above-water emerged and submerged surveys, we defined three types of semi-submerged sea caves: (i) box caves, (ii) joint caves, and (iii) complex caves. Moreover, we added a cave-like landform above the sea level on calcarenous called shelter, or a little extended notch deeply carved into the cliff. The shape mainly depends on the structural and lithological setting of sea cliffs. In the Western sector of the island, we also discovered the only sea cave in Gozo, measuring 122 m in length and 10 m in width, with its floor developing above the mean sea level. This cave base is of interest due to rounded landforms related to marine erosion. In the innermost part of the cave, there is also a beach with rounded pebbles at an elevation of about 7 m asl. Considering the tectonic stability of the island, it could be possibly related to the MIS 5.5 highstand.



Citation: Furlani, S.; Antonioli, F.; Colica, E.; D'Amico, S.; Devoto, S.; Grego, P.; Gambin, T. Sea Caves and Other Landforms of the Coastal Scenery on Gozo Island (Malta): Inventory and New Data on Their Formation. *Geosciences* **2023**, *13*, 164. <https://doi.org/10.3390/geosciences13060164>

Academic Editors: Gang Huang and Jesus Martinez-Frias

Received: 20 April 2023

Revised: 29 May 2023

Accepted: 31 May 2023

Published: 2 June 2023



Copyright: © 2023 by the authors. Licensee MDPI, Basel, Switzerland. This article is an open access article distributed under the terms and conditions of the Creative Commons Attribution (CC BY) license (<https://creativecommons.org/licenses/by/4.0/>).

1. Introduction

Sea caves are very common landforms in areas where there is a steep sea cliff. Wave action weakens the rock masses along joints and faults, enlarging them to form hollows and sea caves [1]. Sea caves occur along all the limestone coasts of the Mediterranean Sea, and as such, various aspects, including biological, geomorphological, and exploration, have been studied. Research results are mainly confined to local papers or proceedings of karst conferences. The volume [2] on Italian marine caves and [3] on Tyrrhenian sea caves discussed and took stock of the current state of knowledge regarding these types of caves. Cave deposits, such as speleothems and other cave deposits, have successfully been used as sea level markers, also in the Mediterranean Sea [4,5].

Sea caves, also known as littoral, coastal, or marine caves, include: (i) sea caves sensu stricto, if they are formed by marine processes, such as biogenic caves, flank margin caves [6,7], and abrasional caves; and (ii) caves that were formed before marine transgression, thus widened by processes such as karstic solution, eolian erosion, tectonic, and volcanic processes [8]. The formation of sea caves is mainly controlled by structural weaknesses, such as layers, cracks, and faults [9,10]. In particular, they begin to form when wave action enlarges a pre-existing weakness of the rock mass, causing selective erosion to produce a hollow [11]. The shape of sea caves depends on the dip of the bedding planes, and the attitude of joints and fault planes [12]. The prerequisites of sea cave formation are the presence of sea cliffs affected by the erosive action of waves and currents [13]. Sea cliffs must contain geological structures that allow selective erosion. The latter can favor the formation of sea caves, sea arches, and sea stacks as part of the coastal scenery [9]. The rock mass must be sufficiently resistant to prevent the formation of pocket beaches at its base and to allow for a sizeable cavity to form without the occurrence of rockfalls [13]. All the pre-requisites for the genesis and development of coastal caves are satisfied on the island of Gozo (Figure 1), where tens of sea caves occur [14,15].

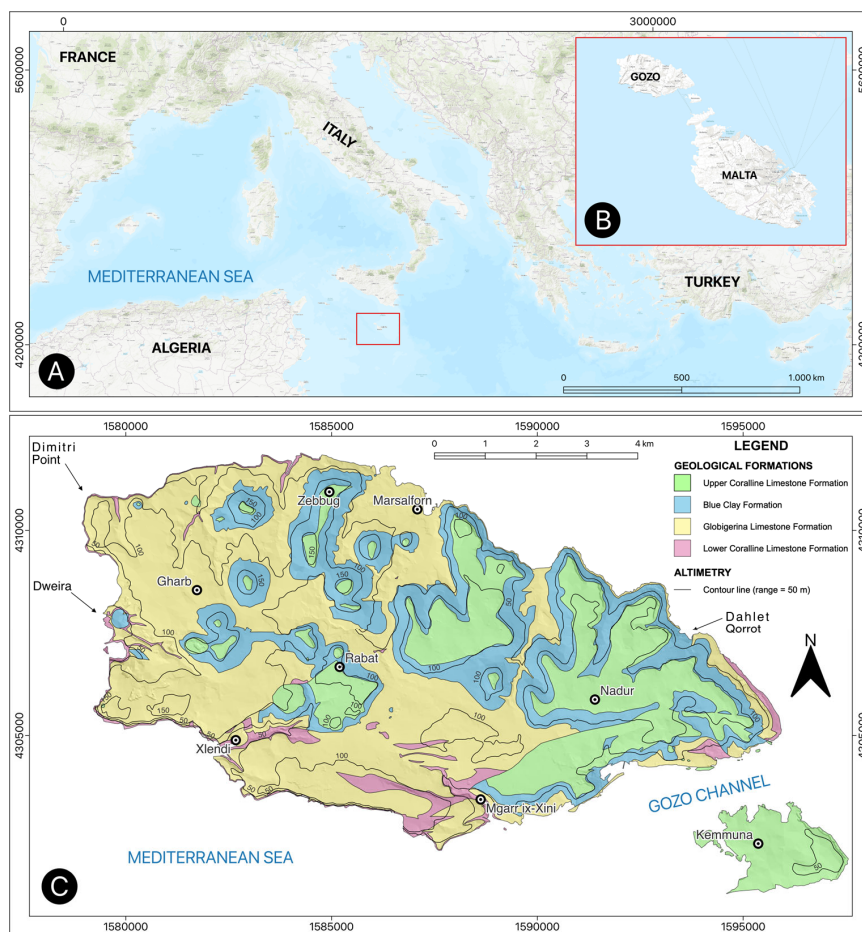


Figure 1. (A) Location of Maltese islands; (B) map of the Maltese islands; and (C) geological map of Gozo, modified from [16].

In this study, we present an inventory of sea caves along the coastline of Gozo, we propose a classification, and, for the first time, we also describe a sea cave with clear evidences of marine landforms above the sea level possibly related to MIS 5.5.

2. Study Area

The Maltese Islands are a group of central Mediterranean islands located in the Sicily Channel (Figure 1), between Sicily (96 km Northward) and the African coasts (about

290 km Westward) [17]. Gozo (65.79 sq.km) is the second-largest island of the Maltese archipelago (Figure 1).

From a geological viewpoint, a sedimentary sequence mainly composed of carbonate rocks spanning in time from the Upper Oligocene to Upper Miocene crops out in Malta and Gozo. Along the coast, four rock types are present in descending order: Upper Coralline Limestone (UCL) Formation (up to 162 m), Blue Clay (BC) Formation (0–65 m), Globigerina Limestone (GLO) Formation (23–207 m), and Lower Coralline Limestone (LCL) Formation (up to 140 m) [17]. According to Schembri [18], GLO rock masses are prevalent in the island of Gozo (Figure 1c). Conversely, LCL rock masses are common along the W coasts of the island.

The island of Gozo has an easterly dip forming high LCL cliffs on the W coast, whilst the N and S coasts of Comino slope gently to the sea, and high cliffs are evident only on the NE coast. The topography of the islands is strongly controlled by an alternation of horsts and grabens developed during the Miocene and Plio-Quaternary extensional stages [16].

Regarding the recent tectonic movements of the Maltese Islands, Furlani et al. [19] investigated some archaeological remains on the mainland of Malta. The research provided an estimation of the relative sea level changes and vertical displacements of Malta since 3.3 ky BP. The submerged structures indicate that their elevations agree with the predicted sea level curve [20], implying relative stability for late Holocene.

2.1. Geomorphological Setting

The coastal geomorphology of the Maltese Islands was investigated by Paskoff and Sanlaville [21], Schembri [18], and Biolchi et al. [22]. The latter identified six morphotypes for the island of Malta: (i) plunging cliffs, (ii) scree coasts, (iii) sloping coasts, (iv) shore platforms, (v) pocket beaches, and (vi) artificial coasts. The coasts of Gozo resulted mainly dominated by plunging cliffs in the S and NW sectors [17], while scree coasts, locally called Rdum, are located in the NE part.

The high plunging cliffs found in the Maltese Islands are composed of LCL rock masses. These cliffs are resistant to weathering and erosion, which allows them to rise up to 90 m above sea level on the SW coast. These cliffs are interrupted by two large coves that correspond to oval sinkholes [23].

Scree-sloping coasts found in the Maltese Islands are characterized by the presence of thousands of UCL boulders. The latter are detached from the cliffs and moved towards the sea due to large slow-moving landslides. These deep-seated landslides and their mechanisms have been investigated in the N part of Malta island by various researchers [24–33]. Recently, Prampolini et al. [34] produced a geomorphological map of the NE coast of Gozo at a scale of 1:15,000 and Rizzo et al. [35] investigated the coastal vulnerability of the above-mentioned sector of the Gozitan coast.

The island of Gozo is primarily characterized by plunging cliffs (46%), low sloping rock (31%), and scree-sloping coasts (20%), with only 3% of sandy deposits. On the other hand, the island of Comino is mainly composed of low sloping rock (60.6%) and cliffs or steep rock face (29.8%). Boulder scree are relatively less dominant compared to Gozo (7.8%) and sandy shores represent only 1.6% of the Comino coastline [18]. Both islands have various karst features, such as semicircular coves and drowned sinkholes [23]. Valleys on the islands are mostly rias that were previously formed by fluvial processes [16,21].

The seabed is deep along the Western part of Gozo where cliffs are high, with depths reaching up to 70 m, while the NE and SE sectors are generally shallower. This information comes from [18,21].

2.2. Climatic and Oceanographic Setting

The climate of the Maltese islands is typically Mediterranean, characterized by hot, dry long summers and mild rainy winters [36]. Weather and climate are strongly influenced by the sea and by the relatively flat morphology of the islands, which does not favor rainfall formation. On average, the island receives 530 mm of rainfall per year [18]. Mean

temperatures range from 12 °C to 27 °C. Due to the central position of the Maltese Islands in the Mediterranean Sea, they are affected by long fetches mainly in the second and fourth quadrant [37]. Dominant winds come from NW [37]. The wave climate around the Maltese Islands is dominated by sea waves rather than swell waves: sea waves, generated by winds in the local area, are characterized by being steep and have relatively short-wave periods when compared to swell waves, which travel into the local area from elsewhere. Tidal oscillations, predominantly semi-diurnal, reach a maximum range of just 20.6 cm on average for spring tides and are reduced to 4.6 cm during neap tides [38].

3. Materials and Methods

The investigation of sea caves along the Gozitan coastline was carried out via swimming surveys in 2013 using the protocol of the Geoswim program [14,39,40]. Data collected were verified in a later campaign in May 2022. In particular, the first survey permitted the location of most of the sea caves presented in this study, while the second survey was aimed at the verification of the 2013 data as well as to perform underwater surveys in selected caves. Another additional survey in October 2022 was carried out in the cave named G32 (see Table 1) at Dimitri Point as sea level markers attributable to MIS 5.5 have been identified within the cave.

The minimum size of sea caves has not been precisely defined, but well-defined hollows at the sea level were mapped. Joints and fractures smaller than approximately 1 m in size were considered as discontinuities enlarged by marine processes.

3.1. Surveys of Sea Caves

Regarding the surveys of sea caves, we present data collected during the 2013 swim survey of the island of Gozo [39], as well as additional punctual surveys both of the submerged (Figure 2A,B) and emergent parts of sea caves (Figure 2C,D).

The 2013 survey followed the Geoswim protocol described by [14,15]. Geoswim consists of swim surveys of selected long sectors of rocky coast, mainly sloping coasts and plunging cliffs [22], with detailed observations of lateral changes in coastal landforms, ecological features of the coast, and mapping of prominent geo-objects.

Instruments, such as GPS, cameras, CTD sensors, echosounder, etc., were fixed onto the instrumental-supported raft (ISR, Figure 2). Two cameras were set in waterproof housings, above and below the ISR, and allowed the collection of ongoing videos and time-lapse images of the coastline being surveyed.

Regarding the DAQ (data acquisition) system, each device was autonomous with respect to the other. The synchronization of data collected during each surveying day was carried out with respect to the Coordinate Universal Time (UTC) and the comparison with GPS coordinates [14,15].

The surveys followed a predetermined route at approximately 1 m to 5 m from the coastline. Small changes in the original routes were caused by nuances in the local topography, and due to the orientation of some of the sea caves [14,15].

Observations were generally reported via radio to the support boat and written in the field booklet, which also includes other navigational information.

The survey covered semi-submerged sea caves, but some submerged caves, noticeable from the surface, were also reported and studied. SCUBA dives were conducted to collect data at eight sea caves using open-circuit dive equipment and underwater cameras.

Morphometric data were acquired in the field using manual instruments for measurements, such as an invar rod or an acoustic distance meter, and also terrestrial photogrammetry (Figure 3) [14,15].

Table 1. List of the sea caves surveyed in Gozo (Malta). The names have been reported when available. The location name refers to the local place names of the sea cliffs. Morphometric parameters which were measured are the following: total length (L), depth at the entrance (D), height at the entrance (H), and width at the entrance (W). All the morphometric parameters are given in meters. The codes of sea caves are reported following the sequence of survey. The table also reports the location of sea arches and sea stacks as part of the coastal scenery.

Cod [#]	Location	Lat	Long	Morphometric Parameters				Type	Lithology	Seafloor	Dive	Notes
				L[m]	D[m]	H[m]	W[m]					
G00	Mgarr ix-Xini	14.272122	36.018691	5	-5	3	5	Joint	LCL	Sand	Y	Small enlarged joint
G01	Mgarr ix-Xini	14.270614	36.0156544					Box	LCL		N	
G02	Mgarr ix-Xini	14.269747	36.015165					Complex	GLO		N	
G03	Ta' Ċenċ Cliffs	14.25591	36.0139207		-18			Joint	LCL	Bedrock	Y	Freshwater
G04	Ta' Ċenċ Cliffs	14.2538125	36.0167085					Joint	LCL		Y	
GS1	Ta' Ċenċ Cliffs	14.2531926	36.0177469	15	-6.8			Submerged	LCL	Bedrock	Y	
G05	Sannat Sunset	14.2444318	36.0189859					Box	LCL		N	Freshwater
G06	Sannat Sunset	14.2416024	36.0191131					Box	LCL		N	
G07	Sannat Sunset	14.2409185	36.0192324					Joint	LCL		N	
G08	Saguna Cliffs	14.2361173	36.0196129					Box	LCL		N	
G09	Saguna Cliffs	14.2341385	36.0200416			7.5	25.5	Joint	LCL		N	
G10	Bardan cliff	14.2284593	36.0217511					Box	LCL		N	
G11	Sanap Cliffs	14.2245791	36.0210436					Joint	LCL		N	
G12	Dana Cliffs	14.2207959	36.0211613		-14	11.5	20	Complex	LCL		N	The sea cave develops along a joint, but the main cave is strata type
G13	Dana Cliffs	14.2195611	36.0213733		-7.3	12	17.7	Complex	LCL	Sand	N	The sea cave develops along a joint, but the main cave is strata type
SA1	Xlendi	14.2160544	36.0239584					Sea arch	LCL		N	
G14	Xlendi	14.2137018	36.0298459					Complex	LCL	Mixed	Y	Xlendi Grotto Tunnel almost entirely submerged at the Xlendi Bay
G76	Xlendi	14.216395	36.03038					Box	LCL		N	Sea cave in the Xlendi harbor
G77	Xlendi	14.215577	36.030131					Box	LCL	Sand	N	Santa Katerina cave
G15	Xlendi	14.2094692	36.0327362	80				Complex	LCL		Y	
GS2	San Raflu Pool	14.2033501	36.0342364	15	-15			Submerged	LCL		N	
G16	San Raflu Pool	14.1986747	36.0334786		-18			Box	LCL	Bedrock	Y	
GS3	Gebel Ben Gorg	14.1942772	36.0329707	0.5	-4			Submerged	LCL		N	
G17	Ras il-Wardija 1	14.1871697	36.0355697					Box	LCL		N	Paleo-cave, freshwater
G18	Ras il-Wardija 2	14.1865132	36.0367578					Box	LCL		N	
G19	Ras il-Wardija 3	14.1897463	36.0400363					Joint	LCL		N	
G20	Dweira	14.1932144	36.0457104					Joint	LCL		N	Freshwater

Table 1. *Cont.*

Cod [#]	Location	Lat	Long	Morphometric Parameters				Type	Lithology	Seafloor	Dive	Notes
				L[m]	D[m]	H[m]	W[m]					
G21	Dweira	14.1933237	36.0462393					Box	LCL		N	
G22	Dweira	14.1931933	36.0468796					Box	LCL		N	Freshwater
SA4	Dwejra	14.189056	36.0541874	25	-5	28	25	Sea arch	GLO		Y	Azure window; it-Tieqa Żerqa. The sea arch collapsed during a storm in March 2017
SA7	Dwejra	14.188699	36.047228					Sea arch	LCL		N	Sea arch at the Fungus rock (Il-Ġebla tal-Ġeneral)
G23	Inland sea	14.189056	36.0541874					Box	GLO		N	
G24	Inland sea	14.1894875	36.0547943					Joint	GLO		N	
G25	Inland sea	14.1898915	36.0548658					Box	GLO		N	
G26	Inland sea	14.1904983	36.0550512		-26	100		Complex	GLO	Bedrock, pebbles	N	Tunnel to inland sea. The cave develops along a vertical joint Well cave
G27	Dwejra	14.1914257	36.055837					Box	GLO		N	
G28	Dwejra	14.1919628	36.0566865	48		26	38	Box	GLO		N	
SA2	Dwejra	14.1911471	36.0591243					Sea arch	GLO		N	
G29	Dwejra	14.1915367	36.0602678					Box	GLO		N	
G30	Dimitri Point	14.1891244	36.0639559	50	-20			Joint	LCL		N	
G31	Dimitri Point	14.1884944	36.0639492		-20			Box	LCL		N	
G32	Dimitri Point	14.1850655	36.0667122	122			20	Box	LCL	Bedrock	Y	The sea cave develops almost completely above the m.s.l. In the innermost part of the cave, a pocket beach is present
G33	Dimitri Point	14.1842833	36.0685285					Joint	LCL		N	
G34	Dimitri Point	14.1840872	36.0713738					Joint	LCL		N	
G35	Dimitri Point	14.1840295	36.0720949					Joint	LCL		N	
G36	Dimitri Point	14.1878795	36.0741022					Joint	LCL		N	
G37	Dimitri Point	14.1900997	36.0742057					Box	LCL		N	
G38	Dimitri Point	14.1916748	36.0739835					Box	LCL		N	
G39	Dimitri Point	14.1936791	36.074132					Box	LCL		N	Freshwater
G40	Dimitri Point	14.194928	36.0746002		-17.9			Box	LCL	Bedrock	Y	
G41	Garbo 1	14.1979927	36.0741818					Box	LCL		N	
G42	Garbo 2	14.1991122	36.0746393	100		14	10	Box	LCL	Bedrock	Y	Ta Cawla
G43	Garbo 2	14.1998981	36.0752509		-15			Box	LCL		N	
G44	Ras il-Reqqa	14.2013965	36.0764104					Box	LCL		N	

Table 1. *Cont.*

Cod [#]	Location	Lat	Long	Morphometric Parameters				Type	Lithology	Seafloor	Dive	Notes
				L[m]	D[m]	H[m]	W[m]					
G45	Ras il-Reqqa	14.2029176	36.0781674					Box	LCL		N	
G46	Ras il-Reqqa	14.2057618	36.0786002					Box	LCL		N	
SA3	Wied Il-Mielaħ	14.2128364	36.0794835		−12.8			Sea arch	LCL		N	Wied Il-Mielaħ Window. Sea arch and cave
G47	Wied Il-Mielaħ	14.2121964	36.0796957					Box	LCL		N	
G48	Wied Il-Mielaħ	14.2130906	36.0794797					Box	LCL		N	
G49	Ponta tar-Reqqa	14.2165452	36.0799805					Box	LCL		N	
G50	Għasri	14.2184774	36.0797239					Box	LCL		N	
G51	Għasri	14.2190333	36.0795673					Box	LCL		N	
G52	Għasri	14.2194306	36.0795876					Box	LCL		N	
G53	Għar tal-Qrewis	14.2209937	36.0796044					Box	LCL		N	
GS4	Għar tal-Qrewis	14.2217333	36.0797591					Submerged	LCL		N	
G54	Wied il-Għasri	14.222664	36.0801764		23.3	10.9		Box	GL		N	Cathedral Cave
G55	Nagħar Il-Baħar	14.2263839	36.0802423		25.3	19.7		Complex	LCL		N	
G56	Nagħar Il-Baħar	14.2270481	36.0803466		11.8	3		Joint	LCL		N	
G57	Nagħar Il-Baħar	14.2277495	36.0804173		16.9	13.5		Box	LCL		N	
G58	Nagħar Il-Baħar	14.2282471	36.0805395					Box	UCL		N	
G59	Nagħar Il-Baħar	14.2312541	36.0819315					Box	GLO		N	
G60	Reqqa Point	14.2355514	36.0811692					Box	LCL/GLO		N	Billinghurst Cave
G61	Dahlet Qorrot	14.3225579	36.0476557					Sea stack	GL		N	
SA5	Għar id-Dorf	14.327939	36.042723					Sea arch	LCL		N	
G62	Għar id-Dorf	14.3298723	36.0408817					Box	LCL		N	
G63	Għar id-Dorf	14.3327781	36.0387429	−7.4				Box	LCL		N	
G64	Ras il-Qala	14.3357926	36.0321026					Box	LCL		N	
G65	Gebel tal-Halfa	14.3309904	36.029055					Joint	UCL		N	
G66	Gebel tal-Halfa—Hondoq	14.3290582	36.0289611					Joint	GLO		N	
G67	Gebel tal-Halfa—Hondoq	14.3253896	36.0282101					Joint	LCL/GLO		N	Lithological contact
G68	Hondoq Bay	14.3216707	36.0265203					Box	GLO		N	Sea cave with pebble beach inside Barbaggan rocks
SA6	Hondoq Bay	14.318761	36.025764					Sea arch	UCL		N	
G69	Tac-Ċaww Rock	14.3164079	36.0260894					Box	UCL		N	
G70	Tac-Ċaww Rock	14.3162483	36.0259872					Box	UCL		N	
G71	Tac-Ċaww Rock	14.3157558	36.0258991					Box	UCL		N	

Table 1. *Cont.*

Cod [#]	Location	Lat	Long	Morphometric Parameters				Type	Lithology	Seafloor	Dive	Notes
				L[m]	D[m]	H[m]	W[m]					
G72	Taċ-Ċawl Rock	14.3155613	36.0258795					Box	UCL		N	
G73	Taċ-Ċawl Rock-Mgarr	14.3134917	36.0267554					Joint	GLO		N	
GS5	Taċ-Ċawl Rock-Mgarr	14.313254	36.0267906					Submerged	GLO		N	
G74	Taċ-Ċawl Rock-Mgarr	14.309694	36.026575		6.5	12		Box	GLO		N	
G75	Xwejni	14.249969	36.079987					Shelter	GLO		N	
G76	Xlendi	14.216395	36.03038					Joint	LCL		N	
G77	Xlendi	14.215577	36.030131					Complex	LCL		N	

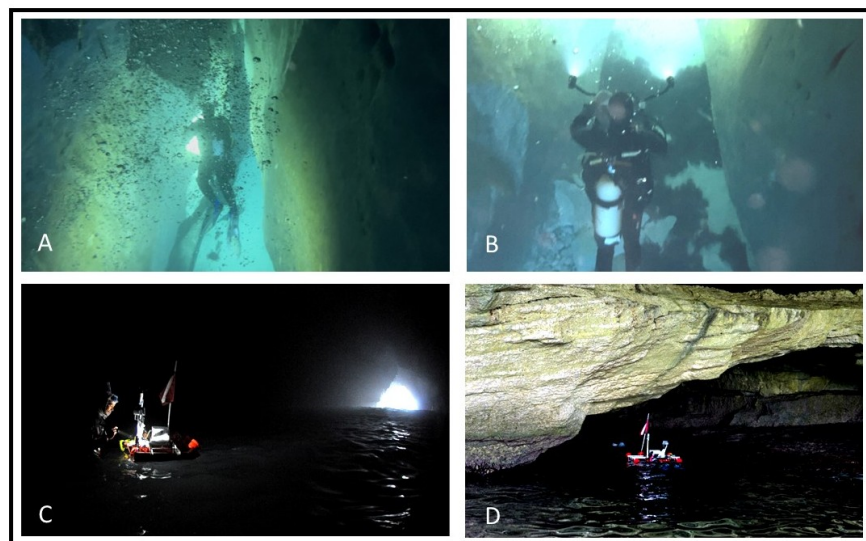


Figure 2. (A,B) SCUBA surveys during the May campaign; (C,D) the ISR used during the Geoswim surveys of the sea caves in Gozo.

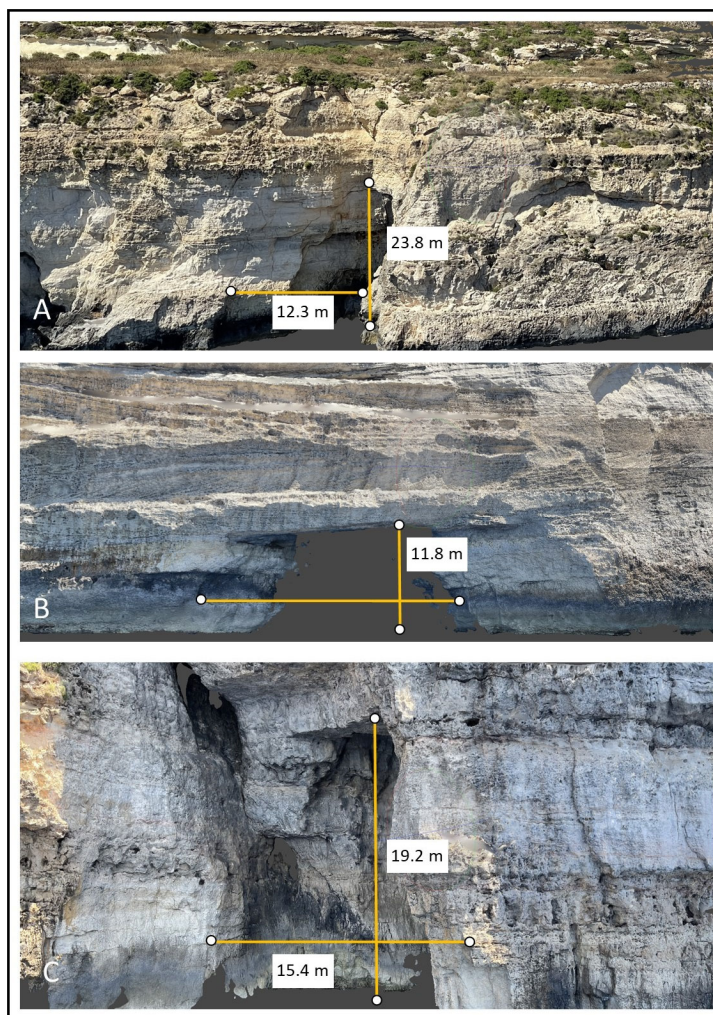


Figure 3. Example of 3D model of sea cave entrances. Sea caves at Gozo: (A) Sea cave#G74 developed along a joint parallel to the coastline; (B) sea cave#G43, developed from collapse of blocks from the roof; (C) sea cave#G33, developed on a joint but evolving for roof collapse. When available, the aforementioned models were used to measure the width and height of the cave entrances.

3.2. Terrestrial Photogrammetry

We performed photographic acquisition to model the inner part of sea cave#G32, and to reconstruct its shape. This approach was also used to obtain the morphometric parameters of the entrances of most of the caves around the island. These high-resolution (HR) images were taken at various elevations roughly perpendicular to the cave walls using a GoPro Hero 7 Black camera. A total of 1522 images were acquired and processed separately in a specialized software used to produce the dense point cloud and 3D model of the cave, according to the DP technique. The first part of DP is known as the SfM technique, and involves the importation of images of each outcrop, and camera alignment.

Collected images were imported in Agisoft MetashapeTM (Agisoft LLC, St. Petersburg, Russia). The latter is a robust software package widely used for the DP technique. The above-cited software includes SfM algorithms that allow the user to align the images and calculate their relative position to each other during the camera alignment phase. The outcome of the camera alignment process was a sparse point cloud of the investigated cave. The second part of DP is known as MVS reconstruction, which involves dense point cloud production, mesh production, and the generation of a 3D textured model (Figure 4). The low-density point cloud is thickened by increasing the number of points, thus generating a dense point cloud. The final processing steps included the production of a 3D surface (mesh) and the generation of 3D textured models.

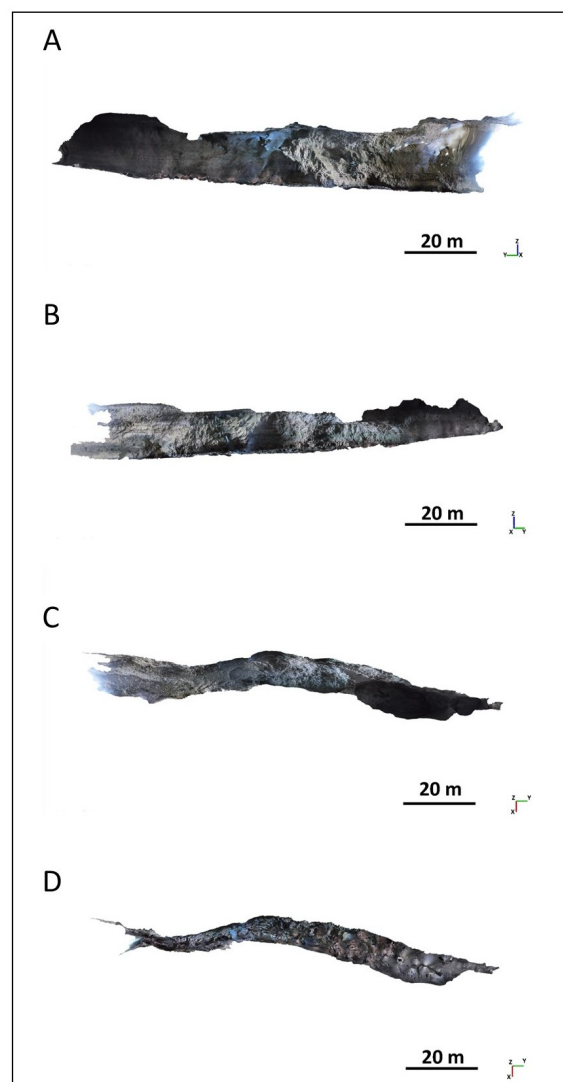


Figure 4. Screenshots of the 3D photogrammetric model of the inner part of sea cave#G32 in the NW sector of Gozo, with orthographic views of (A) S side; (B) N side; (C) top; and (D) bottom.

In a cave environment, global navigation satellite system (GNSS) signals are blocked, so it was not possible to measure the coordinates of the markers to scale the 3D model. Additionally, not having a total station available, it was decided to scale the 3D model within the photogrammetric software by inserting 50 cm scalebars on each side of each of the ten markers positioned along the cave. Moreover, multiple measurements in situ and further checks of the accuracy of the 3D model were made using the point cloud generated via mobile phone (MP) LiDAR as a reference [40].

3.3. iPhone LiDAR Survey

The MP survey aimed to build the 3D model of the innermost part of the G32 cave. We performed two MP surveys using an iPhone 12 Pro MaxTM (Apple Inc., Cupertino, CA, USA) in May and October 2022. These HR images were captured at various elevations roughly perpendicular to the sea cliff. The iPhone 12 Pro MaxTM weighs 0.226 kg, measuring $160.8 \times 78.1 \times 7.4$ mm³, and it is equipped with three rear cameras, including a 12 MP wide-angle, f/1.6, 12 MP ultra-wide-angle, f/2.4, and 12 MP telephoto, f/2.0 with 2/2.5× optical and 10× digital zoom capacity. The 12 MP wide-angle camera was used to capture the images. Our acquisition was conducted within the overhead environment extant in caves, resulting in a very inaccurate GPS signal. The iPhone 12 Pro MaxTM uses a fast stabilization procedure that provides local coordinates within a few tens of seconds. Tavani et al. [41] and Corradetti et al. [42] observed that the accuracy of this model is lower than about 10 m. The acquisition was carried out in automatic mode.

In the cave#G32 (Table 1), we used the MP mounted on a 1.7 m-long selfie stick to extend the LiDAR scanning range that is limited to 5 m. Image acquisition was performed from an average distance of one meter from the cliff face. This distance was selected to guarantee a balance between image quality and the number of images taken. The camera orientation was varied to provide complete and uniform acquisition of the vertical joints that characterize the cliff. Since the cave has heights above 15 m, we integrated the MP LiDAR data with those obtained from the photogrammetric survey (made with the GoPro) to improve the accuracy of the final 3D model.

4. Field Data

Sea caves were mapped and measured as shown in Table 1 and described in detail in the Paragraph 4.1. A separate paragraph is dedicated to sea cave#G32 because it develops almost entirely above the mean sea level and exhibits rounded potholes and channels of possible marine origin.

4.1. Mapping of the Sea Caves and Sea Arches in Gozo

A total of 79 semi-submerged sea caves around the island of Gozo were mapped, 2 of which are tunnels, because they have exits in directions opposite to their entrances. In addition, seven sea arches and five submerged caves (Table 1, Figure 5) were also mapped. Sea cave#G26, also known as the Xlendi Tunnel, is almost totally submerged. We found 64 sea caves along the plunging cliffs of the W sector, between the ria of Mgarr ix-Xini and Reqqa Point in the N side of the island, and 15 sea caves were mapped along the E sector, between Dahlet Qorrot and Tac-Cawl rocks on the S side of the island.

Sea caves in the SW sector mainly develop in LCL rocks, except for the Xlendi tunnel, which opens onto a fault between LCL and GLO. In the Dwejra Bay area on the E side Azure Window, sea caves develop on GLO up to Wied il-Għasri, while at Reqqa Point, sea cave#G1 outcrops. In the E part of Gozo, LCL outcrops between Daleq Qorrot and Qala, the easternmost promontory of Gozo. From the latter site to Tac-Cawl rocks and Mgarr, GLO prevails, but some caves are carved on LCL rock masses (Figure 3).

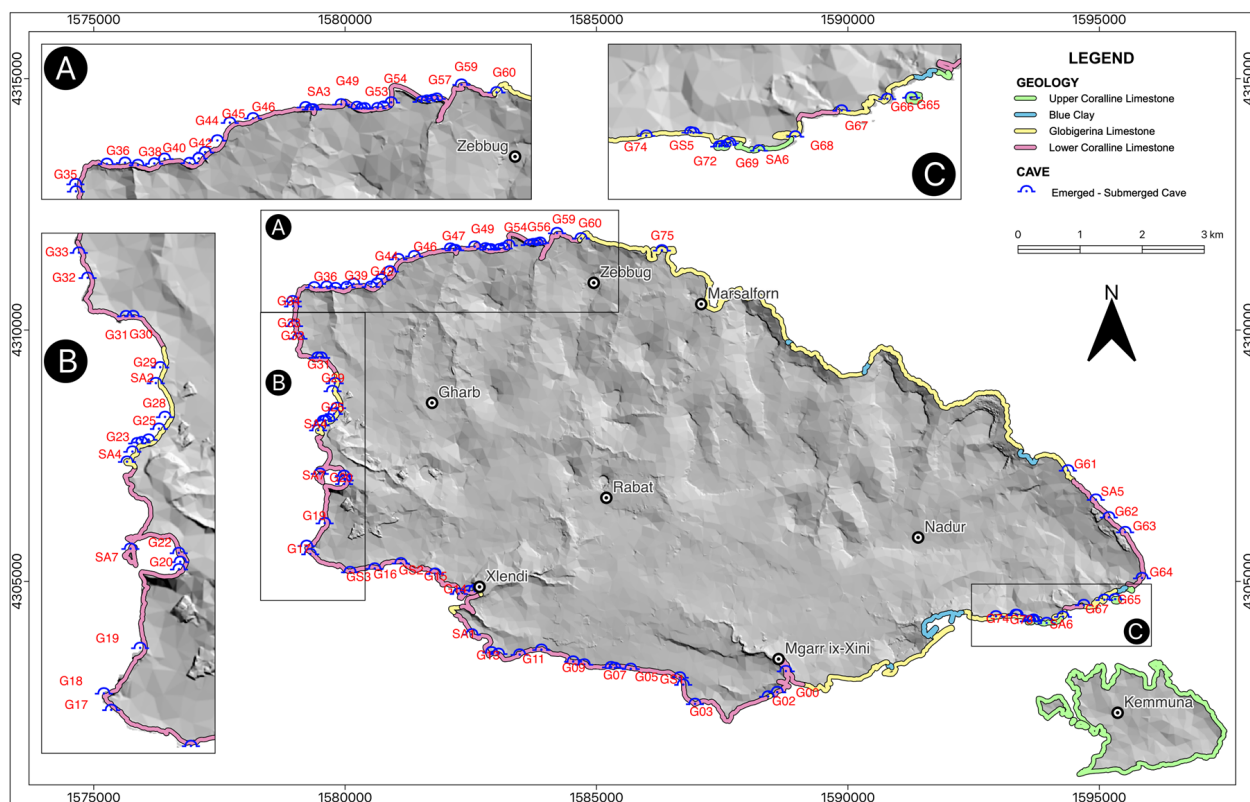


Figure 5. Spatial distribution of sea caves in Gozo. The colored lines represent the lithology outcropping at the sea level. (A) Zoom of the NW part of the island; (B) zoom of the Western sector of the island; (C) zoom of the SW sector of Gozo.

We measured morphometric parameters in 12 caves in the field and confirmed them through DP-derived outputs, while 13 caves were measured solely via photogrammetry. The longest cave is #G32, which is located at Dimitri Point. Finally, we described the sea bottom in six of the caves.

4.2. Sea Cave#G32 with MIS5.5 Landforms and Deposit

Sea cave#G32 has a viable entrance with a height of 16 m (Figure 6), while the floor of the entrance is a few tens of centimeters above sea level (asl). The depth in front of the entrance rapidly increases and the area is partially rocky with sandy deposits. The total length of the cave is 122 m with a maximum width of 10 m. The height of the cave varies between 2.66 m in the innermost part and 15.5 m at the entrance (Figure 7). Here, a large limestone rock partially obstructs the entrance (Figure 8A) and forms a small terrace at about 15 m asl on the left side of the cave. Sea cave#G32 is a long sinuous tunnel roughly elongated in a NW/SE direction. The lower parts of the channels are occupied by seawater. The elevation of the floor increases from 0.5 m to 8.8 m asl in the innermost part. The floor of cave#G32 is generally made of well-rounded potholes as well as of rounded funnels and channels developing in the direction of the cave (Figure 8B,C). Roughly in the middle of the cave, a 30 m long sector of the floor is occupied by collapsed blocks up to 3 m in size. Beyond these blocks, the elevation of the floor increases rapidly. In the innermost sector of the cave, a sandy-to-pebble deposit occurs. The clasts are rounded or sub-rounded up to half a meter in diameter (Figure 8D,E). The deposit lies at an elevation of 8 m asl.

Living organisms occur up to about 40 m from the entrance, mainly on the floor, but also at the wall's foot.

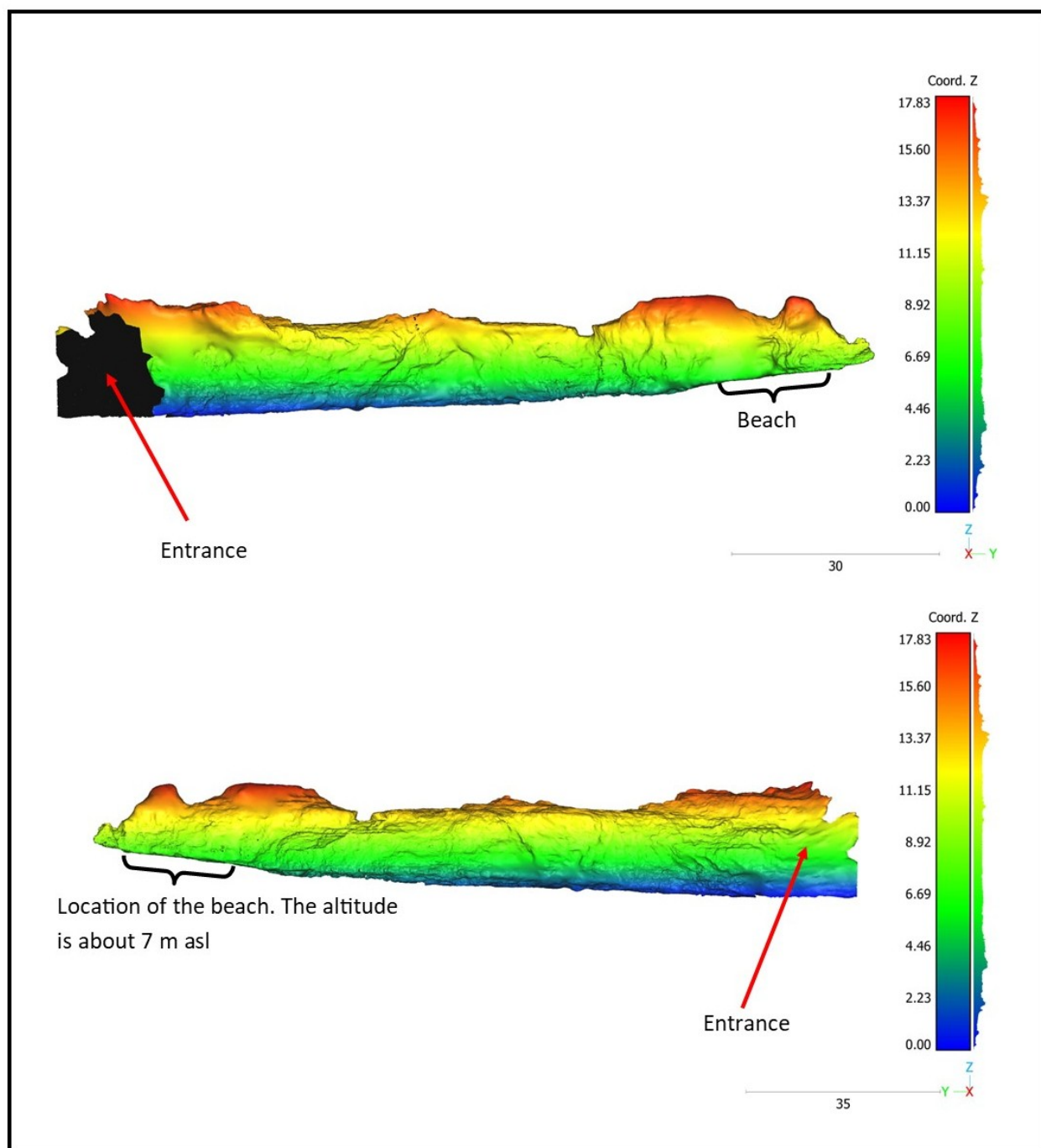


Figure 6. Map of elevation of sea cave#G32 obtained from photogrammetry. The beach in the innermost part of the sea cave lies at 7 m asl and could be remnants of a paleo beach active during MIS5.5.

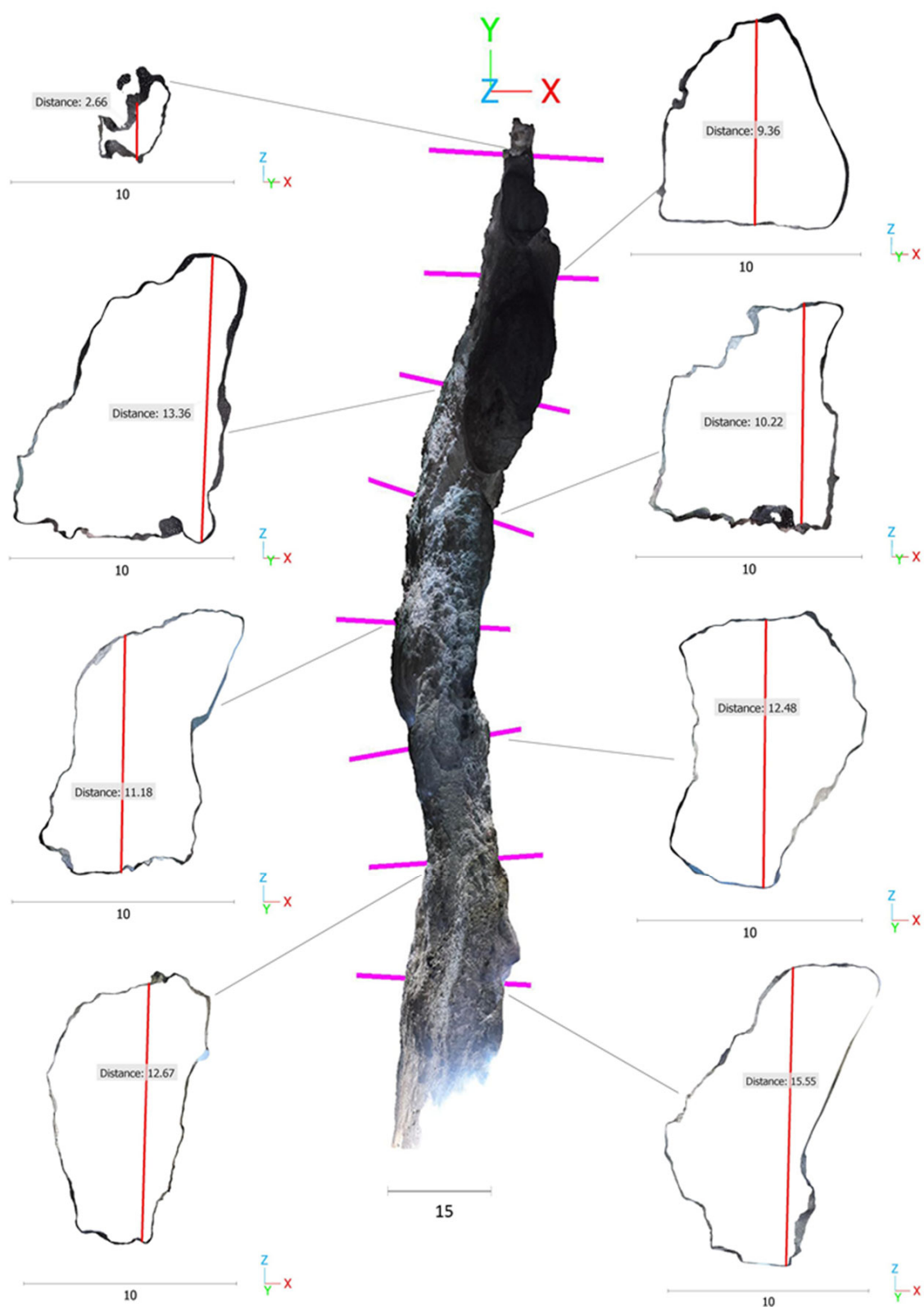


Figure 7. Top view of the 3D model of the sea cave from photogrammetry and 10 cross-sections from the entrance to the innermost part of them.

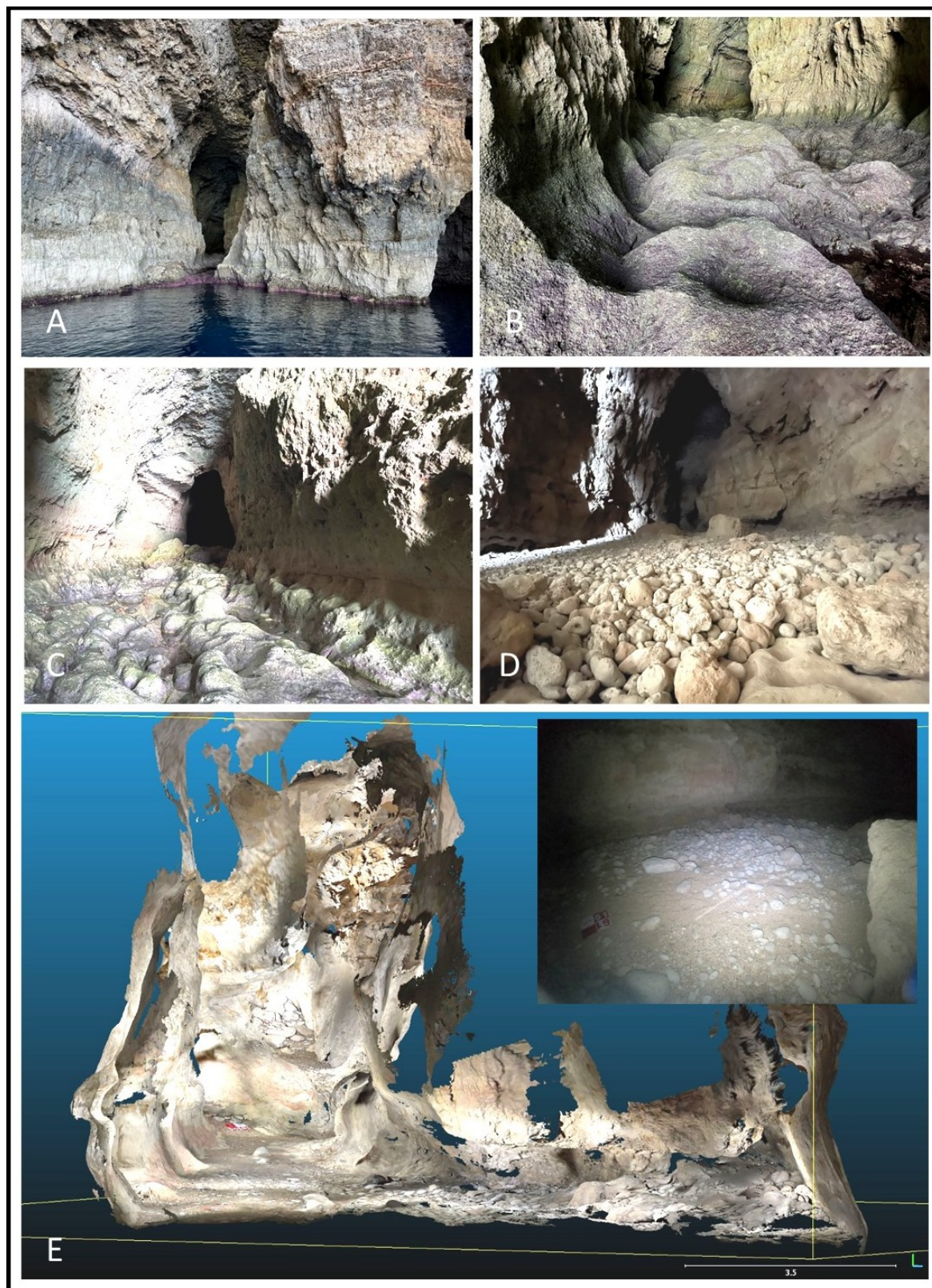


Figure 8. Details of sea cave#G32. (A) View of the entrance; (B) detail of the entrance; (C) the rounded landforms at the base near the entrance; (D) in the background are visible the collapsed blocks; (E) the beach at the innermost sector of the cave and LiDAR model. The beach is composed of rounded and sub-rounded pebbles that stand at about 7 m asl.

5. Discussion

In this section, we discuss the general characteristics of sea caves in Gozo (par. 5.1) and their statistical distribution around the island, the distribution vs. lithology, and the type of sea caves or other surveyed landforms (par 5.2). A separate paragraph (par. 5.3) is devoted to sea cave#G32, as it shows landforms that can be traced back to a paleo sea level.

5.1. Morphometric Characteristics of Sea Caves in Gozo

Sea caves are common landforms along rocky coasts. Their origin and development are due to several factors, such as wave action, karst processes, etc. [1,6,7,9] In Gozo, sea caves can be roughly divided into two main categories mainly according to the shape of the entrance (Table 1).

The first one is the box type, with a squared shape, mainly due to successive collapse of the limestone layers at the roof. The shape of the entrance can be both horizontally enlarged (Figure 9A) or vertically enlarged (Figure 9B).

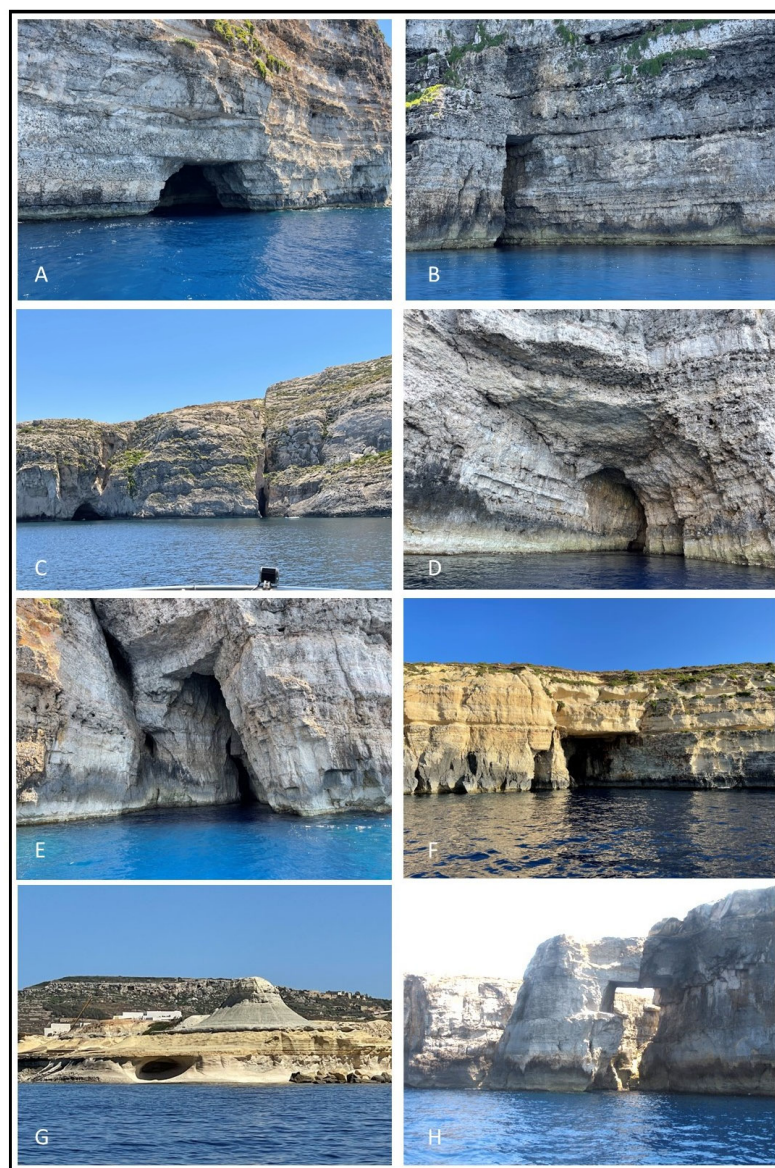


Figure 9. Examples of sea caves in Gozo. (A) Box cave#G16; (B) box cave developed in height; (C) joint cave#G20 and complex box cave#G21 at Dweira; (D) the entrance of sea cave#G32; (E) cave#G34; (F) box cave#G01; (G) the shelter cave#G75 at the base of the butte at Marsalforn; (H) the sea arch#SA3 called Wied Il-Mielah Window.

The second one is the joint type, which develops along vertical or sub-vertical joints in the rock. Jointing can be perpendicular to the sea cliff (Figure 9C) or angled, up to almost parallel (Figure 9D). However, these types represent the end members of a complex mixing of shapes. In fact, many studied sea caves have both a box and joint component simultaneously. For example, they can develop through successive collapses of the roof along a joint (Figure 9E), or at the contact between two different geological formations (Figure 9F). The Xlendi Tunnel is a complex cave that develops on a tectonic contact between the LCL and GLO rock masses, creating a tube that is almost completely submerged and cuts a promontory from one side to the other.

Although submerged sea caves have been reported when visible from the water surface, we did not collect any morphometric parameters. Moreover, we also reported a sea cave in Marsalforn that is carved in the upper member of the GLO rock (#G75). It can be called a shelter, since it looks like a little extended notch carved into the cliff (Figure 9G).

Sea arches are remnant of sea cliff retreat, and possibly of paleo sea caves. We reported seven sea arches 08, but SA4, the famous Azure Window, collapsed during a severe winter storm in 2017 [43]. We also found a sea stack (SS1) near the Azure Window (#SA4) that was probably previously connected to the sea cliff (Figure 9H).

5.2. Sea-Cave Distribution and Lithology

The statistical analysis of the spatial distribution of sea caves along the coastline of Gozo, based on a total amount of 87 coastal landforms, or sea caves, sea arches, and sea stacks showed that 43 (51%) are located on NW part of the island, 16 (19%) on the SE, and 26 (30%) on the SW side. Due to a lack of data, five sea caves were not included in this quantification.

Below the Xwejni rock, there is a shelter carved in the GLO rock mass at Xwejni Bay. It was not considered in the statistical analysis since there is only one cave of this type. Most sea caves ($n = 50$) are box caves (63%), while there are 20 joint caves (26%), 8 complex sea caves (10%), and 1 shelter (1%), as shown in Figure 10B. There are five submerged caves, seven sea arches, and one sea stack. Most of the sea caves developed on LCL rock masses ($n = 56$, 71%), followed by GLO rocks ($n = 15$, 19%) and only a few in UCL rocks ($n = 6$, 8%), and finally at the contact between LCL and GLO ($n = 2$, 2%). Figure 10C shows the percentages for each formation.

The types of sea caves and lithology were compared for each zone of Gozo. In the NW side of Gozo (Figure 10A), most sea caves are located on LCL rocks and are mainly strata-type. In the SE side of Gozo, strata-type caves are also dominant but they are balanced between LCL and UCL (Figure 10B) and are mainly in GLO. In the SW side of Gozo, most of the sea caves are located on LCL, and only one sea cave (Xlendi tunnel) has developed on the contact between LCL and GLO rock masses (Figure 10C). No sea caves have been found on the NE side of the island, where large landslides are abundant [34].

In Gozo, most of the sea caves occur on its W side, spanning from the Northern to Southern sector, while the NE side has no sea caves due to landsliding and lithological factors. For instance, BC terrains outcrop from Marsalforn to Dahleq Qorrot Beach on the NE side of Gozo. Moreover, from Dahleq Qorrot to Hondoq, there are only six sea caves and one sea arch due to the topography of the island, which is mainly characterized by sloping coasts [22]. However, an increasing number of sea caves have developed along the remaining Southern sector towards Mgarr, comprising seven sea caves and two sea arches. No sea caves have been found between Mgarr and Mgarr ix-Xini.

Exposure appears to be the most critical factor, as most of the sea caves have developed along the NW side of the island, which is exposed to the dominant wind (Majjistral). The presence of freshwater at Dweira, as already reported by [44], and on the Southern side of the island, may have also contributed to the development of sea caves in the less-exposed sites.

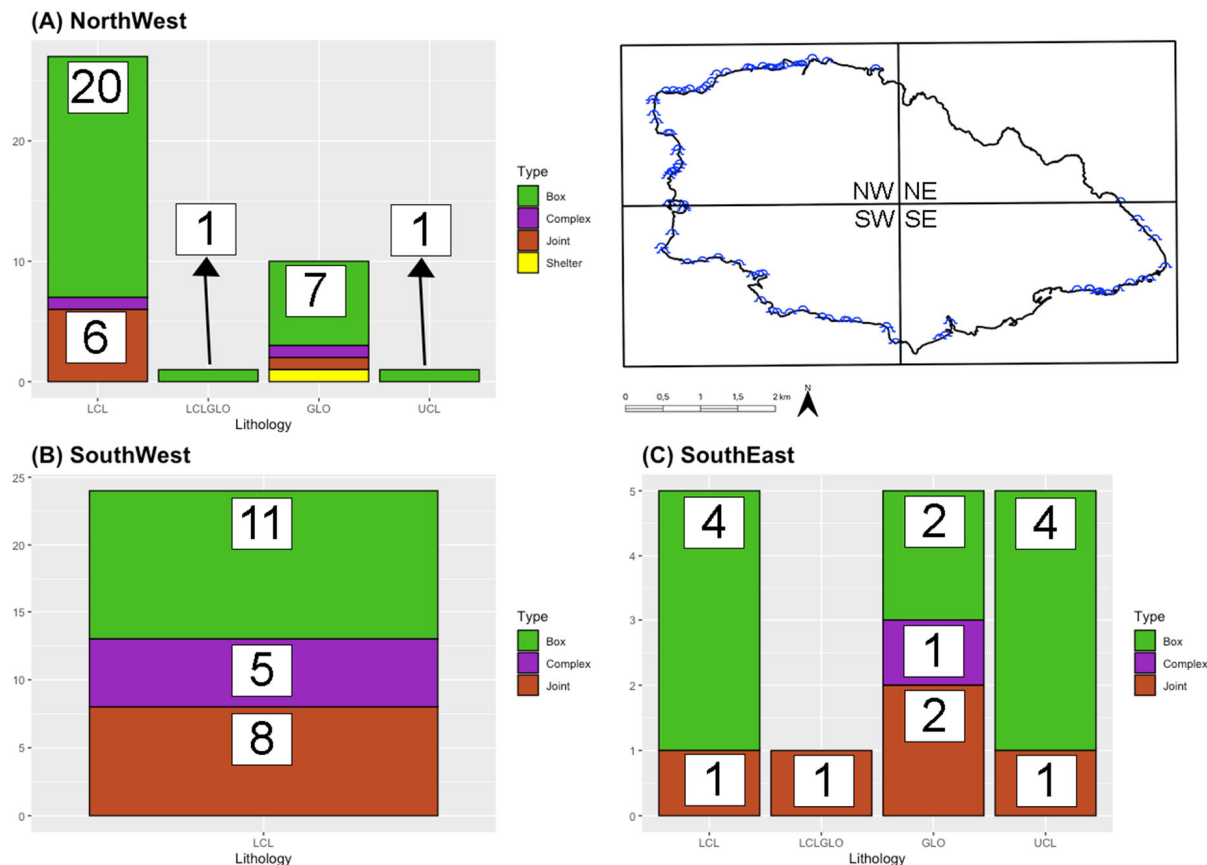


Figure 10. Comparison between sea caves and lithology for each zone of the island. The numbers in the diagrams indicate the sea cave population for different zones (A), types (B), and lithologies (C).

5.3. Sea Cave#G32 and Relative Sea Level Change

Sea cave#G32 is the only cave on Gozo with a floor that has developed almost completely above the mean sea level. Despite this, seawater is still present on the floor, indicating that sea waves can enter the cave during storms up to a few dozen meters inside. Marine processes have significantly shaped the well-rounded channels and potholes, and the foot of the walls is also partially rounded. Moreover, the floor of the cave contains rounded-to-sub-rounded clasts up to the innermost part, where a sandy-to-pebbly deposit occurs. The clasts suggest that the deposit might be a Tyrrhenian beach deposit at an elevation of about 8 m, indicating the tectonic stability of Gozo over a long time, as well as in the Holocene, as reported by [44].

However, no datable fossil remains or even forms of rock biodegradation referable to lithodomies were found, which could be due to the low resistance of the limestones in which the cave is developed. This poor quality of rock masses suggest that these fossils were not preserved over a long time, as reported by [45,46]. The fact that rounded gravels are not cemented could raise doubts, related to the fact that the studied deposit is totally composed by uncemented clasts, and MIS5.5 deposits are usually cemented [44].

Otherwise, the altitude corrected for isostasy of the maximum transgression for MIS 5.5 at Gozo is 8.35 m, as reported by [45], and agrees to the altitude value of inner deposits.

6. Conclusions

A total of 84 sea caves and 8 retreat-related landforms have been investigated for the first time along the Gozitan coasts. These caves had never been inventorized and categorized for their shapes. Most of the caves were box caves ($n = 50$), followed by joint caves ($n = 20$), complex ($n = 8$), and shelter ($n = 1$) thanks to the combination of outputs of the above-water emerged and submerged surveys. All datasets were digitized and stored

in a GIS, revealing that the majority of the sea caves studied developed on LCL rocks. This is likely due to the good quality of rock masses of the above-cited sedimentary rocks. Most of them ($n = 41$; 51%) are located on the most exposed sector (NW), indicating the significant contribution of waves and mechanical factors in their formation and shaping.

Additionally, marine landforms above the mean sea level have been reported in Gozo for the first time. Although dates and lithodomites on the cave walls are not available, the shapes suggest that the deposit found in the innermost part of the cave G32 (Table 1) may be a MIS 5.5 paleo-beach that has been preserved due to its inland location and potential protection from collapsed boulders in the central sector of the cave.

Author Contributions: All authors have contributed to this study. S.F. conceived the paper; S.F., F.A., P.G., E.C. and T.G. performed field surveys; P.G. digitized and stored datasets in GIS; E.C. computed DP; Original idea: S.F. and F.A.; Conceptualization: all authors; Writing—Original draft: all authors; Supervision: S.D. (Sebastiano D’Amico), S.D. (Stefano Devoto) and S.F.; Writing—Review and editing: S.D. (Sebastiano D’Amico), S.D. (Stefano Devoto), F.A. and T.G. All authors have read and agreed to the published version of the manuscript.

Funding: This research received no external funding.

Data Availability Statement: The sea-cave dataset is available on request from the corresponding author.

Acknowledgments: We thank Linley Hastewell (University of Portsmouth) for his comments during the preparation of the manuscript. We are also grateful to three reviewers for their useful comments. This project was supported and funded by the University of Malta (Euro-Mediterranean Centre on Insular Dynamics, Institute of Earth Systems), Department of Mathematics and Geosciences, University of Trieste, and the Geoswim Programme, in addition to Heritage Malta’s Underwater Cultural Heritage Unit for providing the support needed for the 2022 survey.

Conflicts of Interest: The authors declare no conflict of interest. Apple Inc. (Cupertino, California, US) and Agisoft Metashape™ (Agisoft LLC, St. Petersburg, Russia) had no role in the design of the study; in the collection, analyses, or interpretation of data; in the writing of the paper; or in the decision to publish the results.

References

1. Furlani, S.; Cucchi, F.; Biolchi, S. Late Holocene widening of karst voids by marine processes in partially submerged coastal caves (Northeastern Adriatic Sea). *Geogr. Fis. Din. Quat.* **2012**, *35*, 129–140.
2. Alvisi, M.; Colantoni, P.; Forti, P. Grotte marine d’Italia. In *Atti Del Convegno SPELEOMAR 91 E Successivi Contributi; Memorie dell’Istituto Italiano di Speleologia*; Bologna, Italy, 1994; p. 254.
3. Chelli, A.; Pappalardo, M.; Callegari, F. Rapporti fra livelli di carsificazione e paleo-linee di riva nelle isole del Golfo della Spezia (Liguria orientale). In *Atti Della Società Toscana Di Scienze Naturali Residente in Pisa; Memorie, Serie A*; Tuscan Society of Natural Sciences: Pisa, Italy, 2008; pp. 25–37.
4. Antonioli, F.; Furlani, S.; Montagna, P.; Stocchi, P. The Use of Submerged Speleothems for Sea Level Studies in the Mediterranean Sea: A New Perspective Using Glacial Isostatic Adjustment (GIA). *Geosciences* **2021**, *11*, 77. [[CrossRef](#)]
5. Antonioli, F.; Furlani, S.; Montagna, P.; Stocchi, P.; Calcagnile, L.; Quarta, G.; Cecchinelli, J.; Lo Presti, V.; Morticelli, M.G.; Foresta Martin, F.; et al. Submerged Speleothems and Sea Level Reconstructions: A Global Overview and New Results from the Mediterranean Sea. *Water* **2021**, *13*, 1663. [[CrossRef](#)]
6. Mylroie, J.E.; Carew, J.L. The flank margin model for dissolution cave development in carbonate platforms. *Earth Surf. Process. Landf.* **1990**, *15*, 413–424. [[CrossRef](#)]
7. Antonioli, F.; Forti, P. Geologia e genesi delle grotte marine. In *Grotte Marine: Cinquant’anni Di Ricerca in Italia*; Cicogna, F., Bianchi, N.C., Ferrari, G., Forti, P., Eds.; CLEM, Ministero dell’Ambiente, Sezione Difesa Mare: Roma, Italy, 2003; p. 505.
8. Bunnell, D. Littoral caves. In *Encyclopedia of Karst Caves and Karst Sciences*; Gunn, J., Ed.; Fitzroy Dearborn, Taylor and Francis Group: New York, NY, USA, 2004; pp. 491–492.
9. Sunamura, T. *Geomorphology of Rocky Coasts*; John Wiley & Sons: Chichester, UK, 1992.
10. Zezza, F. *Morfogenesi Litorale E Fenomeni D’instabilità Della Costa a Falesia Del Gargano Tra Vieste e Manfredonia; Geologia Applicata e Ingegneria*; Università di Bari-Istituto di Geologia applicata all’Ingegneria: Bari, Italy, 1981; Volume 16, pp. 193–226.
11. Waterstrat, W.J.; Mylroie, J.E.; Owen, A.M.; Mylroie, J.R. Coastal caves in Bahamian eolian calcarenites: Differentiating between sea caves and flank margin caves using quantitative morphology. *J. Cave Karst Stud.* **2010**, *72*, 61–74. [[CrossRef](#)]
12. Guilcher, A. *Coastal and Submarine Morphology*; Methuen: London, UK, 1958; p. 274.
13. Moore, D.G. *Origin and Development of Sea Caves*; National Speleological Society Bulletin: Huntsville, AL, USA, 1954; pp. 71–76.

14. Furlani, S. Integrating observational targets and instrumental data on rock coasts through snorkel surveys: A methodological approach. *Mar. Geol.* **2020**, *425*, 106191. [CrossRef]
15. Furlani, S.; Antonioli, F. The swim-survey archive of the Mediterranean rocky coasts: Potentials and future perspectives. *Geomorphology* **2023**, *421*, 108529. [CrossRef]
16. Pedley, M.; Clarke, M.H. *Limestone Isles in a Crystal Sea: The Geology of the Maltese Islands*; Publishers Enterprises Group: San Gwann, Malta, 2002.
17. Said, G.; Schembri, J.A. Malta. In *Encyclopedia of the World's Coastal Landforms*; Bird, E.C.F., Ed.; Springer: Dordrecht, The Netherlands; Heidelberg, Germany; New York, NY, USA, 2010; pp. 751–759.
18. Schembri, J.A. Coastal Land Use in the Maltese Islands: A Description and Appraisal. Ph.D. Thesis, University of Durham, Durham, UK, 2003. Available online: <http://etheses.dur.ac.uk/4417/> (accessed on 22 March 2023).
19. Furlani, S.; Antonioli, F.; Biolchi, S.; Gambin, T.; Gauci, R.; Lo Presti, V.; Anzidei, M.; Devoto, S.; Palombo, M.; Sulli, A. Holocene sea level change in Malta. *Quat. Int.* **2013**, *288*, 146–157. [CrossRef]
20. Lambeck, K.; Antonioli, F.; Anzidei, M.; Ferranti, L.; Leoni, G.; Scicchitano, G.; Silenzi, S. Sea level change along the Italian coast during the Holocene and projections for the future. *Quat. Int.* **2011**, *232*, 250–257. [CrossRef]
21. Paskoff, R.; Sanlaville, P. Observations geomorphologiques sur les cotes del'archipel Maltais. *Z. Fur Geomorphol.* **1983**, *22*, 310–328.
22. Biolchi, S.; Furlani, S.; Devoto, S.; Gauci, R.; Castaldini, D.; Soldati, M. Geomorphological identification, classification and spatial distribution of coastal landforms of Malta (Mediterranean Sea). *J. Maps* **2016**, *12*, 87–99. [CrossRef]
23. Calleja, I.; Tonelli, C. Dwejra and Maqluba: Emblematic Sinkholes in the Maltese Islands. In *Landscapes and Landforms of the Maltese Islands*; Gauci, R., Schembri, J.A., Eds.; Springer: Cham, Switzerland, 2019; pp. 129–139.
24. Devoto, S.; Biolchi, S.; Bruschi, V.M.; Furlani, S.; Mantovani, M.; Piacentini, D.; Pasuto, A.; Soldati, M. Geomorphological map of the NW Coast of the Island of Malta (Mediterranean Sea). *J. Maps* **2012**, *8*, 33–40. [CrossRef]
25. Panzera, F.; D'Amico, S.; Lotteri, A.; Galea, P.; Lombardo, G. Seismic site response of unstable steep slope using noise measurements: The case study of Xemxija Bay area, Malta. *Nat. Hazards Earth Syst. Sci.* **2012**, *12*, 3421–3431. [CrossRef]
26. Mantovani, M.; Devoto, S.; Forte, E.; Mocnik, A.; Pasuto, A.; Piacentini, D.; Soldati, M. A multidisciplinary approach for rock spreading and block sliding investigation in the north-western coast of Malta. *Landslides* **2013**, *10*, 611–622. [CrossRef]
27. Soldati, M.; Barrows, T.T.; Prampolini, M.; Fifield, K.L. Cosmogenic exposure dating constraints for coastal landslide evolution on the Island of Malta (Mediterranean Sea). *J. Coast. Conserv.* **2018**, *22*, 831–844. [CrossRef]
28. Soldati, M.; Devoto, S.; Prampolini, M.; Pasuto, A. The spectacular landslide-controlled Landscape of the Northwestern Coast of Malta. In *Landscapes and Landforms of the Maltese Islands*; Gauci, R., Schembri, J.A., Eds.; Springer: Cham, Switzerland, 2019; pp. 167–178.
29. Devoto, S.; Macovaz, V.; Mantovani, M.; Soldati, M.; Furlani, S. Advantages of Using UAV Digital Photogrammetry in the Study of Slow-Moving Coastal Landslides. *Remote Sens.* **2020**, *12*, 3566. [CrossRef]
30. Colica, E.; D'Amico, S.; Iannucci, R.; Martino, S.; Gauci, A.; Galone, L.; Galea, P.; Paciello, A. Using unmanned aerial vehicles photogrammetry for digital geological surveys: Case study of Selmun promontory, northern Malta. *Environ. Earth Sci.* **2021**, *80*, 1–14. [CrossRef]
31. Devoto, S.; Hastewell, L.J.; Prampolini, M.; Furlani, S. Dataset of Gravity-Induced Landforms and Sinkholes of the Northeast Coast of Malta (Central Mediterranean Sea). *Data* **2021**, *6*, 81. [CrossRef]
32. Mantovani, M.; Bossi, G.; Dykes, A.P.; Pasuto, A.; Soldati, M.; Devoto, S. Coupling long-term GNSS monitoring and numerical modelling of lateral spreading for hazard assessment purposes. *Eng. Geol.* **2022**, *296*, 106466. [CrossRef]
33. Colica, E.; Galone, L.; D'Amico, S.; Gauci, A.; Iannucci, R.; Martino, S.; Pistillo, D.; Iregbeyen, P.; Valentino, G. Evaluating Characteristics of an Active Coastal Spreading Area Combining Geophysical Data with Satellite, Aerial, and Unmanned Aerial Vehicles Images. *Remote Sens.* **2023**, *15*, 1465. [CrossRef]
34. Prampolini, M.; Gauci, C.; Micallef, A.S.; Selmi, L.; Vandelli, V.; Soldati, M. Geomorphology of the north-eastern coast of Gozo (Malta, Mediterranean Sea). *J. Maps* **2018**, *14*, 402–410. [CrossRef]
35. Rizzo, A.; Vandelli, V.; Buhagiar, G.; Micallef, A.S.; Soldati, M. Coastal Vulnerability Assessment along the North-Eastern Sector of Gozo Island (Malta, Mediterranean Sea). *Water* **2020**, *12*, 1405. [CrossRef]
36. Groove, T.; Rackman, O. *The Nature of Mediterranean Europe. An Ecological History*; Yale University Press: New Haven, CT, USA, 2001; p. 384.
37. Galdies, C. *The Climate of Malta: Statistics, Trends and Analysis, 1951–2010*; Valletta National Statistics Office: Valletta, Malta, 2011; p. 45. Available online: https://nso.gov.mt/en/publications/Publications_by_Unit/Documents/B3_Environment_Energy_Transport_Agriculture_Statistics/The_Climate_of_Malta.pdf (accessed on 18 April 2023).
38. Drago, A. Sea level variability and the 'Milghuba' seiche oscillations in the northern coast of Malta, Central Mediterranean. *Phys. Chem. Earth* **2009**, *34*, 948–970. [CrossRef]
39. Furlani, S.; Antonioli, F.; Gambin, T.; Gauci, R.; Ninfo, A.; Zavagno, E.; Micallef, A.; Cucchi, F. Marine notches in the Maltese Islands (central Mediterranean Sea). *Quat. Int.* **2017**, *439*, 158–168. [CrossRef]
40. Luetzenburg, G.; Kroon, A.; Bjørk, A.A. Evaluation of the Apple iPhone 12 Pro LiDAR for an Application in Geosciences. *Sci. Rep.* **2021**, *11*, 22221. [CrossRef] [PubMed]
41. Tavani, S.; Billi, A.; Corradetti, A.; Mercuri, M.; Bosman, A.; Cuffaro, M.; Seers, T.; Carminati, E. Smartphone assisted fieldwork: Towards the digital transition of geoscience fieldwork using LiDAR-equipped iPhones. *Earth-Sci. Rev.* **2022**, *227*, 103969. [CrossRef]

42. Corradetti, A.; Seers, T.; Mercuri, M.; Calligaris, C.; Busetti, A.; Zini, L. Benchmarking Different SfM-MVS Photogrammetric and iOS LiDAR Acquisition Methods for the Digital Preservation of a Short-Lived Excavation: A Case Study from an Area of Sinkhole Related Subsidence. *Remote Sens.* **2022**, *14*, 5187. [[CrossRef](#)]
43. Caruana, J.; Wood, J.; Nocerino, E.; Menna, F.; Micallef, A.; Gambin, T. Reconstruction of the collapse of the ‘Azure Window’ natural arch via photogrammetry. *Geomorphology* **2022**, *408*, 108250. [[CrossRef](#)]
44. Furlani, S.; Antonioli, F.; Gambin, T.; Biolchi, S.; Formosa, S.; Lo Presti, V. Submerged speleothem in Malta indicates tectonic stability throughout the Holocene. *Holocene* **2018**, *28*, 1588–1597. [[CrossRef](#)]
45. Antonioli, F.; Ferranti, L.; Stocchi, P.; Deiana, G.; Lo Presti, V.; Furlani, S.; Marino, C.; Orrù, P.; Scicchitano, G.; Trainito, E.; et al. Morphometry and elevation of the last interglacial tidal notches in tectonically stable coasts of the Mediterranean Sea. *Earth-Sci. Rev.* **2018**, *185*, 600–623.
46. Furlani, S.; Vaccher, V.; Antonioli, F.; Agate, M.; Biolchi, S.; Boccali, C.; Busetti, A.; Caldarerì, F.; Canziani, F.; Chemello, R.; et al. Preservation of Modern and MIS 5.5 Erosional Landforms and Biological Structures as Sea Level Markers: A Matter of Luck? *Water* **2021**, *13*, 2127. [[CrossRef](#)]

Disclaimer/Publisher’s Note: The statements, opinions and data contained in all publications are solely those of the individual author(s) and contributor(s) and not of MDPI and/or the editor(s). MDPI and/or the editor(s) disclaim responsibility for any injury to people or property resulting from any ideas, methods, instructions or products referred to in the content.